Investigation of the Physical Structure of the Primary Plant Cell Wall by Proton Magnetic Resonance†

Alex L. MacKay,‡ Julia C. Wallace,‡,§ Ken Sasaki,§ and Iain E. P. Taylor*,§

Department of Physics, University of British Columbia, Vancouver, British Columbia V6T 2A6, Canada, and Department of Botany, University of British Columbia, Vancouver, British Columbia V6T 2B1, Canada

Received June 30, 1987; Revised Manuscript Received October 16, 1987

ABSTRACT: Primary cell walls prepared from the actively extending region of *Phaseolus vulgaris* L. etiolated seedling hypocotyls were examined by proton nuclear magnetic resonance (^{1}H NMR). The second moment (M_{2r}) of the free induction decay (FID), the interpair second moment ($M_{2interpair}$), and dipolar (T_{1D}), transverse (T_2), and spin–lattice (T_1) relaxation times were measured. Two components can be distinguished from the FID, one which is associated with the protons from the cell wall polymers and the other which is from ^{1}H^{2}HO. The measured M_{2r} of the restricted fraction, 5×10^9 s^{-2}, when compared to the estimated rigid lattice second moment, indicated that the components of the bean cell wall were almost rigid on the NMR time scale. Measurements of T_{1D} and $M_{2interpair}$ indicated that the primary cell wall molecules were divided into two domains: the more rigid made up 64% of the mass or 74% of the protons and consisted of cellulose and hemicellulose; the second component contained pectin and some hemicelluloses. Three T_2 components were separated: the longest was associated with the free water; the shorter two components corresponded to water undergoing motion which was affected by the cell walls. A cell wall model is presented which is consistent with the results. A microfibrillar core of cellulose (100–400 Å) is surrounded by a layer of hemicellulose with a thickness of 20–80 Å. Attached to this rigid core are the pectic and some hemicellulosic molecules, which undergo much more motion.

The general view of the plant primary cell wall as a composite material made up of cellulose microfibrils in a matrix of hemicelluloses, pectic polysaccharides, protein, and water is well established [for reviews, see Fry (1986), MacNeil et al. (1984), Taiz (1984), and Preston (1979)]. Most of our detailed knowledge of primary cell wall structure is based upon the extensive research which has been carried out on wall chemistry [for example, MacNeil et al. (1984) and van Holst et al. (1980)]. The application of this considerable chemical information to a quantitative architectural model requires knowledge of the microscopic physical properties of the constituent polymers. However, the heterogeneity of the wall makes it very difficult to interpret physical measurements on a molecular level. For example, X-ray diffraction, which is most useful for systems with periodic architecture, can give information about structure within the microfibril but cannot resolve periodic structure within the rest of the cell wall. Electron microscopy measurements, which are done without water, can give estimates of microfibrillar dimensions but little information on structure within the matrix.

The nuclear magnetic resonance (NMR) technique is very sensitive to local structure and dynamics on a molecular level. Accordingly, there have been many NMR studies of the physical properties of biological samples such as proteins (Brown et al., 1981), peptides (Pauls et al., 1984), and membranes (Davis, 1983) and of whole cells (Bloom et al., 1986). The main difficulties in applying NMR techniques to the cell wall are the inherent inhomogeneity of the samples and the fact that most of the constituents are long polymer molecules which do not readily give rise to resolved NMR spectra.

Despite these difficulties, useful data have been obtained with various NMR approaches. High-resolution ^{13}C NMR of cell wall polysaccharide extracts dissolved in organic solvents (Joseleau & Chambert, 1984) can provide information on the chemical structure of the most abundant polysaccharides. High-resolution solid-state ^{13}C cross-polarization magic angle spinning (CPMAS) NMR spectroscopy has been applied to many carbohydrate systems (Pfeffer, 1984). CPMAS studies of cellulose have provided information on crystallinity (Horii et al., 1984; Atalla & VanderHart, 1984) and structural details at the unit-cell level (Atalla & VanderHart, 1984) and, when applied to wood, on the relative amounts of the cellulose, hemicellulose, and lignin constituents (Haw et al., 1984).

Proton NMR studies have been carried out on cellulose (Harai et al., 1980; MacKay et al., 1985, 1982) and on plant cell walls (Taylor et al., 1983; MacKay et al., 1982). We found (MacKay et al., 1985) that ^{1}H NMR moment and relaxation measurements can provide details on cellulose morphology and are sensitive to the state of crystallinity of the polymer chains.

In the present study, several ^{1}H NMR methods have been applied to primary plant cell walls prepared from the hook region of the etiolated hypocotyl of bean (*Phaseolus vulgaris* L.) seedlings. The aim was to distinguish and analyze the NMR signals from physically different components of the cell wall in order to obtain a quantitative picture of the structure and dynamics of the major molecular constituents.

Relevant NMR Concepts. Since the NMR methods employed in this work are different from those conventionally applied to carbohydrate systems, we present an explanation of the basic concepts and the rationale behind them. For a more complete and rigorous treatment, we refer the reader to the well-known treatise by Abragam (1961).

The ^{1}H NMR line shape in plant cell walls is dominated by the dipolar interactions between neighboring protons, which are represented by H_D. In the absence of molecular motion, the ^{1}H spectrum consists of a broad featureless line which can be characterized most quantitatively by its spectral moments.

† Supported by NSERC of Canada.
‡ Department of Physics.
§ Department of Botany.

0006-2960/88/0427-1467$01.50/0

The second moment M_2 is particularly useful since it is simply related to the spatial arrangement of protons in the sample and is given, for a powder, by

$$M_2 = (9/20)\gamma^4\hbar^2(1/N)\sum_j \sum_{j\neq k} 1/r_{jk}^6 \quad (1)$$

where γ is the proton gyromagnetic ratio, $\hbar$ is Planck's constant divided by 2π, N is the number of protons, and r_{jk} is the separation between proton j and proton k.

It is convenient to separate cell wall motions into either of two limiting time scales—slow motions characterized by a correlation time $\tau_c \gg M_2^{-1/2}$ and fast motions with $\tau_c \ll M_2^{-1/2}$. Hydrogen nuclei that undergo only slow motions give rise to "rigid lattice" NMR spectra, with a seond moment as in eq 1. With the onset of fast molecular motions, the dipolar interaction, H_D, undergoes rapid fluctuations about an average value $\langle H_D \rangle$, and a narrower "motionally averaged" NMR spectrum results. Although the true second moment, M_2, is independent of motion, the measured second moment, known as the residual moment M_{2r}, is smaller and can be used to investigate the nature of rapid molecular motion in cell walls.

Rapid fluctuations in H_D, in addition to reducing the apparent second moment by an amount $\Delta M_2 = M_2 - M_{2r}$, also give rise to an exchange of energy between the molecular motion and the nuclear spin transitions. This process, known as spin relaxation, can provide valuable information on the amplitude and frequency of molecular motions in the cell wall samples.

As a result of its coupling to the molecular motions through the dipolar interactions, the total nuclear magnetization of the cell wall samples comes to equilibrium with the external magnetic field H_0 at a rate characterized by the spin–lattice relaxation time T_1. T_1 is sensitive to the spectral density of molecular motions at frequencies ω_0 and $2\omega_0$, where ω_0 is the Larmor frequency, γH_0, which is 90 MHz for our ^{1}H NMR measurements.

Another kind of relaxation that can be measured is the decay of transverse magnetization. Decay that occurs because of the distribution of precession frequencies is characterized by a time T_2^*, and that due to the finite lifetime of the spin states is characterized by the spin–spin relaxation time T_2. The different molecular constituents of cell walls have a very wide range of transverse relaxation times, ranging from tens of microseconds for T_2^* of cellulose to hundreds of milliseconds for T_2 of free water.

Yet another type of relaxation process measurable by ^{1}H NMR is the establishment of an equilibrium of the spins in the local magnetic fields of the neighboring nuclei. This type of relaxation, which can only be determined for spins having a nonzero value of $\langle H_D \rangle$, is characterized by the time constant T_{1D} and is sensitive to molecular motions in a frequency range near ω_D, corresponding to the dipolar spectrum of the spins. For the cellulose microfibrils, $\omega_D \simeq 10^5$ Hz.

For spins that have a nonzero average dipolar interaction, $\langle H_D \rangle$ a proportion of the magnetization can be refocused by the two-pulse solid-echo sequence (Mansfield, 1965; Boden & Mortimer, 1973). For spins that experience a wide range of dipolar couplings, or, more simply, a strong coupling and a set of weaker couplings, the decay of the solid echo with pulse separation is determined by the smaller couplings. It is convenient to separate the dipolar couplings at each proton into two contributions: the strongest dipolar coupling (i.e., that from the nearest-neighbor proton)—which gives the spectrum its overall width— and all the other dipolar couplings—which tend to "dephase" the strongest coupling. The second moment of the line shape, eq 1, can therefore be separated into two components, $M_{2intrapair}$ and $M_{2interpair}$, which are defined as

$$M_2 = M_{2intrapair} + M_{2interpair} = (9/20)\gamma^4\hbar^2(1/N)\sum_j 1/r_{jl}^6 + (9/20)\gamma^4\hbar^2(1/N)\sum_j \sum_{k\neq j,l} 1/r_{jk}^6 \quad (2)$$

where r_{jl} refers to the separation between proton j and its nearest-neighbor proton l.

In any NMR relaxation experiment on an inhomogeneous system like the plant cell wall, there is always a possibility of magnetization transfer between different sample domains. If, during a measurement, one component of the sample approaches equilibrium with the lattice at a different rate than that of another component, then nonuniformities in spin temperature will develop in the sample. However, these components can come into equilibrium with each other (i.e., establish a common spin temperature) via a spatial propagation of magnetization known as spin diffusion, which is characterized by the spin diffusion constant D, which may be estimated, for a solid, by (Goldman, 1970)

$$D = a^2 M_2^{1/2}/30 \quad (3)$$

where a^2 is the mean squared interproton spacing. The presence of spin diffusion in cell wall samples can make it difficult to measure relaxation of individual molecular components. However, if a model of the component structures is available, the rate of spin diffusion between components may provide estimates of domain dimensions.

Techniques for Fractionation of Cell Wall NMR Signal on a Physical Basis. The plant cell wall is a very inhomogeneous system on both a physical and a chemical level, and different components of the wall have different ^{1}H NMR properties. The NMR signals from hydrogens with different physical environments can be distinguished by a variety of techniques that are based on the following rationale.

The usual ^{1}H NMR spectrum, obtained by Fourier transformation of the free induction decay (FID) following a 90° pulse contains equal contributions from all protons in the sample. Any NMR parameter measured from the total FID, for example M_{2r}, is therefore an average property of the entire sample. Since the T_2 values for protons in the more solid parts of the cell wall are several orders of magnitude smaller than those of the free water, it is possible, by inspection, to distinguish contributions to the FID due to the more solid parts of the wall from those due to the more mobile parts of the wall. However, we use a more quantitative approach to subdividing the NMR signal into components.

The hydrogens in our cell wall samples can be unambiguously separated into two classes—one with nonzero average dipolar interaction (i.e., $\langle H_D \rangle \neq 0$) and the other with zero average dipolar interaction ($\langle H_D \rangle = 0$). Physically, the former component undergoes either anisotropic motion or no motion on the ^{1}H NMR time scale of 10^{-5} s, and the latter component experiences isotropic motion on the same time scale. We label these two components of the wall respectively as the restricted fraction and the mobile fraction.

By use of the Jeener–Broekaert pulse sequence (Jeener & Broekaert, 1967), $[90_0-\tau_1-45_{90}-\tau_2-45_{90}]$, an echo is generated only for those spins with $\langle H_D \rangle \neq 0$. Provided that the spacing between the first two pulses τ_1 is sufficiently short (Bloom et al., 1977), the Jeener echo shape, even for inhomogeneous samples, is the first derivative of the FID from these spins. Then, by integration of the Jeener echo, an FID can be generated from the restricted fraction of the cell wall alone.

The solid echo sequence $[90_0-\tau-90_{90}]$ also produces an echo only for those spins possessing nonzero $\langle H_D \rangle$. For short τ,

the signal from spins with zero $\langle H_D \rangle$ is unaffected by the second pulse. Then, provided that the restricted fraction decays in time 2τ but the mobile fraction does not decay in this time, if an FID (beginning at time 2τ before the echo peak) is subtracted from the solid echo, the resulting signal should be from the restricted fraction alone.

The Jeener and solid echo sequences enable us not only to isolate the NMR signal from the restricted fraction of our cell wall samples but also to characterize this fraction further by M_{2r}, T_{1D}, and $M_{2interpair}$ measurements. Obviously, the restricted fraction may contain several different components.

The mobile fraction of the cell wall samples may be investigated with the Carr–Purcell–Meiboom–Gill (CPMG) (Carr & Purcell, 1954; Meiboom & Gill, 1958) pulse sequence, which refocuses any decay of the spins due to magnetic inhomogeneity or chemical shift differences but does not refocus the signal from the restricted fraction of the sample. With the CPMG sequence, we are able to further compartmentalize the mobile fraction of the sample on the basis of T_2.

Experimental Procedures

Sample Preparation. Bean seeds (*Phaseolus vulgaris* L. cv Top Crop Green Pod) were obtained locally and were germinated in moistened vermiculite at 23 °C in the dark. Seedlings were harvested when the lengths of the hypocotyls were 12–15 cm (7–8 days).

The hypocotyl segments (the first 2 cm below the cotyledon insertion) were ground, washed in H_2O to remove cytoplasm, extracted with 80% ethanol, and treated with α-amylase (hog pancreas, Sigma type I-A) (Sasaki & Taylor, 1986, 1984). The cell wall residue was lyophilized, suspended in ^2H_2O (99.7 atom % ^2H) and lyophilized again. The sample was transferred to a 10 mm diameter NMR test tube and rehydrated in excess ^2H_2O.

Total Sugars in the Cell Wall. The cell wall was dissolved by treatment with 72% H_2SO_4 at 23 °C for 3 h, diluted with H_2O, and centrifuged. The supernatant solution was assayed for the total sugar by the phenol–sulfuric acid method (Ashwell, 1966) with glucose as a standard.

Total Sugars and Total Uronic Acids in the TFA-Insoluble Fraction of the Cell Wall. The cell wall was hydrolyzed with 2 N trifluoroacetic acid (TFA) at 120 °C for 2 h. The lyophilized TFA-insoluble residue was dissolved in 72% H_2SO_4 at 23 °C for 1 h, diluted with H_2O, and centrifuged. The supernatant solution was assayed for total sugars by the phenol–sulfuric acid method with glucose as a standard and for total uronic acids with galacturonic acid as a standard (Blumenkrantz & Asboe-Hansen, 1973).

To obtain more chemical information, segments were excised when hypocotyls were 10 cm long, frozen to −40 °C, homogenized to a powder in a Sorvall Omnimixer, and disrupted twice in an Edebo X-press (Biotec Inc., Rockville, MD). The broken cells were thawed, dispersed by sonic disruption, washed with water until no cytoplasmic contamination was visible under dark-field light microscopy, and boiled in 80% ethanol (3 times for 1 h). Residual starch was removed by treatment with α-amylase (Taylor & Sasaki, 1986). The preparation was washed in water and lyophilized. Wall material (100 mg) was digested with 30 mL of ammonium oxalate/oxalic acid (0.25% w/v of each) 5 times for 1 h at 80 °C (to remove most pectic polysaccharide), then with 30 mL of 4% (w/v) KOH twice for 24 h at room temperature (to remove hemicellulose I), and then with 10 mL of 24% KOH twice for 24 h at 5 °C (to remove hemicellulose II). The residual wall material (cellulosic fraction) was washed with water to neutral pH and lyophilized between extraction steps.

NMR Methods. All of the ^1H NMR measurements were taken at 24 °C on a Bruker SXP 4-100 pulse NMR spectrometer operating at 90 MHz. Data were acquired on a Nicolet digital oscilloscope. The supervision of the data collection was performed by a μVAX I microcomputer, which was also used for data processing. A locally built pulse programmer was used to control the experiments. Details on the pulse programmer, data acquisition, and processing have been described elsewhere (Sternin, 1985).

The 90° pulse length ranged between 2.5 and 3.5 μs, and the receiver deadtime following the pulse was 10 μs. The free induction decay (FID) following each $90°_0$ pulse was collected. Signal to noise was improved by inserting $180°_0$ pulses 5 ms before every second 90° pulse and subtracting the resulting signal from memory. To compensate for the dephasing due to the inhomogeneity of the magnetic field, the FID following the first $90°_0$ pulse was refocused by a series of $180°_{90}$ pulses. The repetition rate for each experiment was 10 s ($6T_1$), allowing the system to reach equilibrium before the subsequent sequence of pulses was applied.

For the measurement of the interpair second moment, $M_{2interpair}$, the time τ between the two 90° pulses in the pulse sequence $[90_0–\tau–90_{90}]$ was varied between 10 and 90 μs, and the maximum of the resulting solid echo was recorded. The contribution to the echo from the residual FID due to protons with very small or zero average dipolar coupling was removed by first subtracting the FID following a single 90° pulse. A small correction was then applied to the resulting signal to compensate for the FID from protons with nonnegligible average dipolar coupling. Again to improve signal to noise, a $180°_0$ pulse was applied 10 ms before every second solid echo and single 90° pulse sequence, and the resulting signals were subtracted from and added to memory, respectively. For a single $M_{2interpair}$ component, the echo maximum should follow the relation (Boden & Mortimer, 1973)

$$E(\tau) = E(0) \exp[(-9/16)M_{2interpair}\tau^2] \quad (4)$$

The echo maximum occurred at $2\tau + 2$ μs, and the echo height averaged over 4 μs was plotted against τ^2 to evaluate $M_{2interpair}$.

For the dipolar relaxation measurements the Jeener–Broekaert echo pulse sequence, $[90_0–\tau_1–45_{90}–\tau_2–45_{90}]$, was applied with τ_1 fixed at 10 μs and τ_2 varying between 1 and 90 ms. The phase of the second pulse was alternated between 90° and 270°, and the signal after the third pulse was alternately added to and subtracted from memory to minimize the contribution of the FID to the Jeener echo at short τ_2 values.

For exponential dipolar relaxation

$$A_D(\tau_2,t) = A_D(0,t) \exp(-\tau_2/T_{1D}) \quad (5)$$

where $A_D(\tau_2,t)$ is the height of the Jeener echo at a time t following the third pulse. The echo maximum occurred between $t = 14$ and $t = 18$ μs, and the mean echo height between these two times was plotted against τ_2 for the determination of T_{1D}.

T_2 measurements were made with the CPMG pulse sequence, $[90–\tau/2–(180–\tau)_n]$, where $\tau = 200$ μs. The average amplitude of the peak following each 180° pulse was taken over four points.

An inversion recovery pulse sequence was used for the spin–lattice relaxation measurements. A 180° pulse was applied at a time τ before every second 90°, and alternate scans were subtracted from the accumulated signal in memory. For exponential relaxation

$$A(\tau,t) = A(0,t) \exp(-\tau/T_1) \quad (6)$$

where $A(\tau,t)$ is the FID intensity at a time t following the 90°

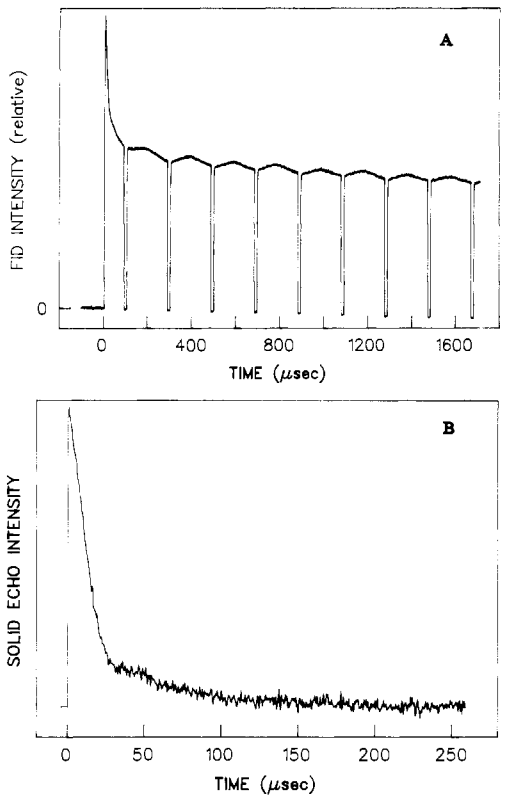

FIGURE 1: Free induction decay (FID) of the bean cell wall sample. (A) FID of rigid and more mobile components (a series of $180°_{90}$ pulses were inserted to refocus any dephasing of the mobile component due to magnetic field inhomogeneities) and (B) decay of the solid echo (τ = 12 μs).

pulse. The time τ was varied between 10 ms and 3 s, and the intensity (averaged over six points) between 14 and 600 μs following the 90° pulse was measured as a function of τ.

To investigate cross-relaxation between domains, the Goldman–Shen experiment, $[90_0-\tau_1-90_{180}-\tau_2-90_0]$, was performed with τ_1 = 150 μs and a range of τ_2 values from 1 ms to 3 s. To remove T_1 effects, on alternate scans the second pulse was 90_0 and the signal was subtracted from the cumulative memory.

The data analyses for $M_{2\text{interpair}}$, T_{1D}, T_2, and T_1 involved fitting sums of exponential functions to the experimental data. It should be noted that this is a nontrivial procedure. In this study, the nonlinear functional minimization program MINUIT (James & Roos, 1975) was employed in a χ^2 minimization analysis. Confidence limits of 68% were obtained for the parameter estimates.

RESULTS

The FID of the bean cell wall sample is shown in Figure 1A. By refocusing of the FIDs with a series of $180°_{90}$ pulses, the separation between the different components is less ambiguous. The rapidly decaying fraction, ($T_2^* < 200$ μs), corresponds to motionally restricted protons whereas the fraction that decays more slowly, ($T_2^* > 200$ μs), can be identified with mobile protons. The rapidly decaying fraction consists of two subfractions, one with T_2^* of about 30 μs which contributes most of the intensity and the other with T_2^* of about 80 μs.

The signal was calibrated by adding a known amount of ^1H in water to the sample and obtaining the FID. When an FID was obtained from the vacuum-dried bean cell wall sample, the component with T_2^* of 80 μs was absent, and the proportion of protons contributing to the restricted fraction increased to 100%.

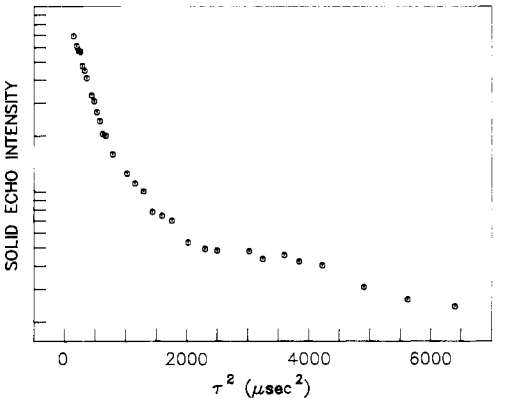

FIGURE 2: Spin-pair dipolar echo decay. The amplitude of the solid echo peak is plotted against the square of the time between the two 90° pulses.

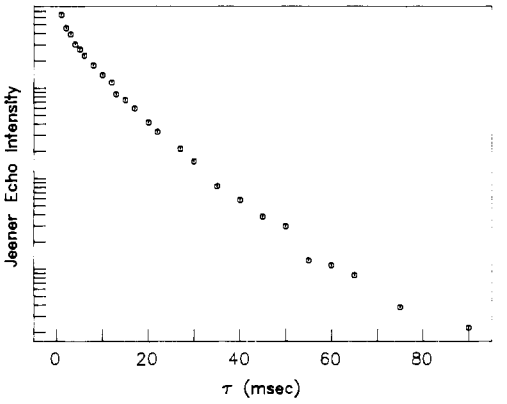

FIGURE 3: Dipolar relaxation of bean cell walls. The Jeener echo amplitude is plotted against the time between the two 45° pulses.

From the decay of the FID of the hydrated sample, we found the second moment, M_{2r}, of the restricted fraction to be 5×10^9 s^{-1}. We have assumed that the M_{2r} for the mobile protons is negligible.

Figure 1B shows the decay of the solid echo taken at τ = 12 μs. The signal to the left of the peak maximum was zeroed to facilitate comparison with Figure 1A.

Figure 2 shows the decay of the solid echo as a function of the square of the time between the two 90° pulses. By use of the MINUIT routine described previously, this curve can be well fitted by the sum of two exponentials (see eq 4). The resulting $M_{2\text{interpair}}$ values and their relative proportions are listed in Table I.

In Figure 3 the Jeener echo amplitude as a function of τ_2 is shown. This decay curve was fitted to two exponentials, both having the form given by eq 5. It should be noted that contributions to the signal from the FID were nonnegligible at $\tau_2 < 2$ ms, and therefore these points were not included in the fit. The dipolar relaxation times (T_{1D}) and the relative proportions of the two components are shown in Table I. The shape of the Jeener echo was not highly dependent on τ_2.

The integral of the Jeener echo at τ_1 = 10 μs, τ_2 = 3 ms is shown in Figure 4. For short τ_2, the integral of the Jeener echo should be proportional to the FID, and indeed, it compares closely with the shape of the FID of the restricted fraction of the protons in Figure 1A. This indicates that there is no component that has a short T_2^* and zero average dipolar interactions.

The first point in the CPMG curve (Figure 5) was 600 μs after the preparation pulse, and the signal was collected until it had decayed to less than 1% of the initial intensity. The curve was well fitted by the sum of three exponential com-

Table I: Relaxation Times and Moments for the Motionally Restricted Fraction and Relaxation Times for the Motionally Mobile Fraction of Bean Cell Wall Preparations

(A) Relaxation Times and Moments for the Motionally Restricted Fraction of Bean Cell Wall Preparations[a]

NMR quantity measured	value	restricted fraction (%)	assignment
T_2^* (μs)[b]	30	80	cellulose + hemicellulose II
	80	20	pectin + hemicellulose I
M_{2r} (10^9 s^{-2})	5		total cell wall (dry)
$M_{2interpair}$ (10^9 s^{-2})	4.46 (4.29–4.64)	74.3 (73.2–75.5)	cellulose + hemicellulose II
	0.18 (0.16–0.21)	25.7 (24.6–26.8)	pectin + hemicellulose I
T_{1D} (ms)	12.6 (10.5–14.3)	65 (51–79)	paracrystalline cellulose + hemicellulose + pectin
	35.8 (29.8–48.1)	35 (21–49)	crystalline cellulose
T_1 (s)	1.68 (1.63–1.74)		total cell wall (dry)

(B) Relaxation Times for the Motionally Mobile Fraction of Bean Cell Wall Preparations[a]

NMR quantity measured	value	mobile fraction (%)	assignment
T_1 (s)	0.21 (0.20–0.23)		water (average)
T_2 (ms)	4.5 (4.0–5.0)	19 (18–20)	water of hydration
	99.0 (84.4–115.3)	27 (26–29)	wall-associated water
	952.0 (921–988)	54 (52–55)	free water

[a] The ranges in parentheses represent 68% probability limits for the relaxation times, moments, and proportions. [b] From integrated Jeener echo.

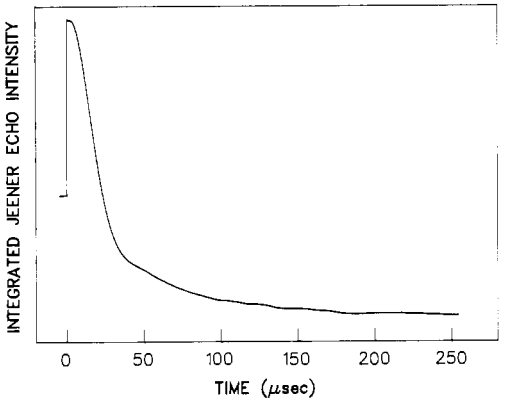

FIGURE 4: Integrated Jeener echo intensity, which represents the free induction signal from those protons with nonzero average dipolar interaction (dry cell wall components).

ponents, and the corresponding T_2 values are listed in Table I.

Figure 6 shows the two decay curves of the FID, 14 and 600 μs, following the 90° pulse of the inversion recovery sequence as a function of τ. The former curve can be represented by two exponentials of the form given by eq 6. From inspection of the FIDs, the two exponentials, with T_1s of 1.6 and 0.21 s, could be identified with the restricted and mobile fractions of the sample, respectively. The latter curve could be fitted to a single exponential with T_1 = 0.21 s.

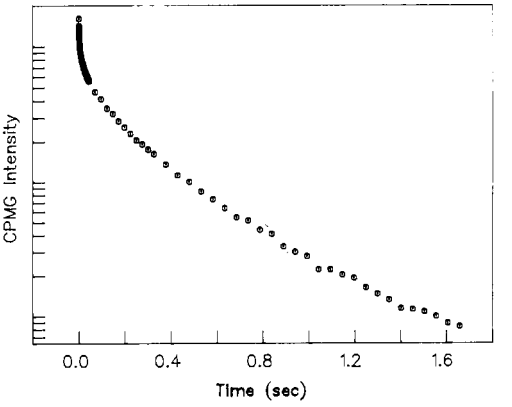

FIGURE 5: Carr–Purcell–Meiboom–Gill (CPMG) decay curve, which represents the signal from those protons with zero average dipolar interaction (water).

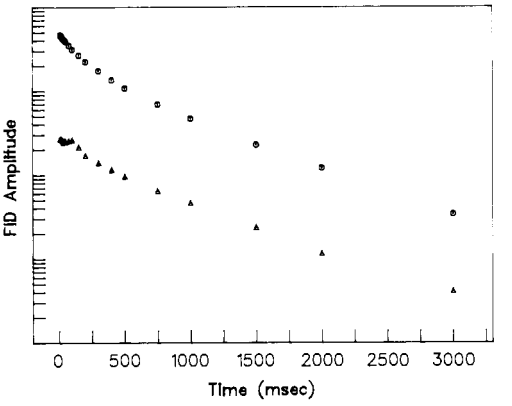

FIGURE 6: Spin–lattice relaxation. The FID amplitude is plotted against the time between the 180° and 90° pulses. The (○) and (△) points were measured from the FID at 14 and 600 μs, respectively, so that the former represents all the protons and the latter the water protons.

Table II: Chemical Fractionation of the Bean Cell Wall Preparation

component of bean cell wall	chemical fractionation procedure	percentage of whole wall mass	percentage contribution to ^{1}H NMR signal
total sugars	phenol–H_2SO_4	100	
total sugars minus TFA-insoluble fraction	2N TFA soluble removed and residue analyzed with phenol–H_2SO_4	49.6	
pectin	ammonium oxalate digestion	18.0	21
hemicellulose I	4% KOH digestion	25.8	19
hemicellulose II	24% KOH digestion	13.2	14
cellulosic fraction	remaining component	43.0	46

A Goldman–Shen experiment was performed to determine whether cross-relaxation occurred between the two fractions. There was no substantial cross-relaxation over times up to 3 s, indicating that the restricted and mobile fractions are uncoupled from each other on that time scale.

The chemical fractionation of the bean cell wall preparations is presented in Table II. We show the percentage of the total cell wall (by weight) remaining after the hydrolysis or digestion steps.

The TFA-insoluble fraction corresponds almost quantitatively to the cellulosic fraction remaining after oxalate and KOH extraction. The polymer composition presented is representative of similar analyses of wall preparations from

the same hypocotyl region that we have done in the last 5 years. Cell wall protein, whether enzymic or structural, is not resolved chemically because we are unable to distinguish the protein ^1H NMR signal from that of polysaccharides. Trace uronic acids were detected in the cellulosic fraction.

Discussion

Spin Bookkeeping. It is convenient to separate the molecules of the primary cell wall into five major classes (MacNeil et al., 1984; Taiz, 1985; Preston, 1979): cellulose, hemicellulosic polysaccharides, pectic polysaccharides, protein, and water. Analysis of the ^1H NMR results requires determination of the distribution of protons among these components. Since the ^1H NMR signal from water would normally overwhelm that from the cell wall components other than water, our wall samples have been prepared in ^2H_2O. Some of the cell wall hydrogen nuclei can exchange with deuterons in the water and therefore not contribute to the ^1H NMR signal. In the cell wall, we expect that the hydrogens at electronegative sites of loosely packed polysaccharide chains will exchange with hydrogens of water but that in the interior of crystalline aggregates such as the cellulose microfibrils exchange of hydrogens on electronegative sites will not occur (Mackay et al., 1985). Table II lists the approximate relative proportions and number of protons for the major classes of cell wall polysaccharide components. The chemical fractionation procedure separated the cell walls into cellulosic, hemicellulosic, and pectic fractions. Proteins make up about 5% of the mass of the cell walls and may be distributed between all fractions. We have assumed that none of the cellulose or hemicellulose II hydrogens can exchange with the water and that all of the exchangeable pectic and hemicellulose I hydrogens do. Other models for hydrogen exchange would yield only slightly different proportions.

The Free Induction Decay. The ^1H FID in Figure 1A contains equal contributions from all protons in the bean cell wall sample. As noted under Results, two components can be readily distinguished on the basis of their decay rate, T_2^*. The component with the faster decay rate ($T_2^* < 200$ μs) is associated with protons on molecules undergoing restricted motion, and the other component ($T_2^* \gg 200$ μs) is associated with protons on much more mobile molecules.

Due to the hygroscopic nature of the dry cell wall samples, it is difficult to predict accurately or to control the $^1H^2HO$ contribution to the signal. We have therefore calibrated the FID intensity in terms of number of protons by adding a known amount of ^1H_2O to the sample and measuring the increase in signal. The result, that the total number of protons contributing to the FID in Figure 1B is 2.3×10^{21}, when compared with Table I indicates that the FID component with shorter T_2^* has approximately the same number of protons as the dry cell wall sample which had a mass of 62.3 mg. Furthermore, we found that when all the water was removed by drying in vacuo, the entire FID had a short decay constant and that addition of $^1H^2HO$ led to increased intensity only for the more mobile component. This strongly implies that the FID component with the shorter T_2^* is from protons on the dry cell wall molecules and the other component is from $^1H^2HO$. For bean cell walls the M_{2r} value for the restricted fraction of 5×10^9 s^{-2} should be compared to rigid lattice second moments for the component molecules, which are 7.3×10^9 s^{-2} for cellulose and hemicellulosic molecules and 3.5×10^9 s^{-2} for pectic polysaccharides (MacKay et al., 1982). Using Table II and the property that all protons contribute equally to M_2, we estimate the rigid lattice M_2 of the cell wall sample to be 6.8×10^9 s^{-2}. We therefore conclude that, on average, the restricted fraction of bean primary cell walls undergoes very little motion on the ^1H NMR time scale.

Dynamic Primary Cell Wall Structure. We can make several specific and quantitative statements about the dynamic molecular structure in our preparations of bean hypocotyl cell walls.

(i) *The primary cell wall molecular components (not including water) are either rigid or undergo anisotropic motion on the ^1H NMR time scale of 10^{-5} s.* This important conclusion follows from the results that, for short times between pulses, the solid echo or the integral of the Jeener echo has the same shape as the part of the FID with the rapid decay time. This means that there are no contributions to the FID from isotropically reorienting molecules possessing short T_2^* values such as loosely bound oligomers.

(ii) *On the basis of their motion, the primary cell wall molecules (not including water) can be divided into two fractions. The larger component which makes up 74% of the wall signal and is practically rigid consists of all the cellulose and some of the hemicellulosic molecules. The other component, which undergoes much more motion, consists largely of pectic polysaccharide and some hemicellulosic molecules.*

The first component is characterized by an $M_{2\text{interpair}}$ of 4.5×10^9 s^{-2} and the second by an $M_{2\text{interpair}}$ of 1.8×10^8 s^{-2}. Since the second component has a much smaller $M_{2\text{interpair}}$ than the first, it should also have a much smaller M_{2r}. In fact, we note from Figure 1B that the rapidly decaying fraction of the FID is the sum of these two components, the former with a T_2^* of 30 μs and the latter with a longer T_2^* of 80 μs. Assuming the smaller component makes a negligible contribution to the total M_{2r}, we calculate that the larger component possesses an M_{2r} value of about 7×10^9 s^{-2}. Crystalline cellulose has an M_2 and $M_{2\text{interpair}}$ of 7.3×10^9 and 4.0×10^9 s^{-2}, respectively (MacKay et al., 1984). We note also that the pectic polysaccharides, with an M_2 of 3.5×10^9 s^{-2}, could not contribute appreciably to the larger component. We therefore conclude that the larger component contains the cellulose microfibrils. However, since the cellulosic fraction itself can contribute a maximum of 46% to the signal, the larger component must also contain some hemicellulosic molecules, presumably the hemicellulose II fraction.

The smaller component must contain the pectic polysaccharides plus some other molecules, presumably the hemicellulosic I fraction. The rigid lattice $M_{2\text{interpair}}$ for the pectic molecules is about 1.8×10^9 s^{-2}, and for hemicellulosic molecules it is larger. Then, the measured value of 1.8×10^8 s^{-2} indicates the presence of motional averaging at a rate faster than 100 kHz and with amplitudes large enough to reduce the second moment by an order of magntiude.

(iii) *Phaseolus vulgaris L. primary cell wall cellulose is physically similar to cellulose from chemical cotton or filter paper.* Previous studies of cellulose from cotton and filter paper (MacKay et al., 1985) have indicated the presence of a "paracrystalline" component with an M_2 of 5.4×10^9 s^{-2}, an $M_{2\text{interpair}}$ of 2×10^9 s^{-2}, and a T_{1D} of 8 ms. This component was associated with loosely packed fibrils of cellulose which can undergo restricted motion. Dipolar relaxation studies of our primary cell wall samples indicated two domains: one with 35% of the intensity and a T_{1D} of 35 ms and the other with 65% of the intensity and a T_{1D} of 13 ms. By comparison, we associate the former component with crystalline cellulose and the second with all the other wall polymer molecules including paracrystalline cellulose. This interpretation leads to the conclusion that primary wall cellulose is approximately 70% crystalline (or more so if spin diffusion processes occur on this

time scale). Electron diffraction and X-ray studies of the cellulose microfibrils in other primary cell wall systems have suggested a lower crystallinity (Chanzy et al., 1979).

(iv) *The cellulose microfibrils of bean primary cell walls have diametric dimensions between 100 and 400* Å. Because we measure two different T_{1D} values, the two corresponding cell wall fractions must exist in domains which are sufficiently far apart that spin diffusion processes do not bring them to the same spin temperature. Using eq 3 and the values of M_2 and T_{1D} for the crystalline cellulose and assuming cylindrical symmetry, we can put a lower limit on the microfibrillar diameter of about 100 Å. Since the two fractions do have a common T_1 value of about 1.6 s, spin diffusion processes apparently do result in a common temperature in this time. This places an upper limit on the microfibrillar diameter of about 400 Å. A distribution of microfibrillar diameters may be present.

Water and the Primary Cell Wall. Water plays an important role in the dynamic structure of the primary cell wall. In fact, the FID component with T_2^* of 80 μs, which we associate with more fluid regions of the cell wall, was found to become much more rigid upon lyophilization. Our CPMG measurements on the cell wall water (^2H_2O + $^1H^2HO$) can be accurately fitted by the sum of three exponentials, which correspond to T_2 values of 4.5, 99, and 952 ms with amplitudes of 19%, 27%, and 54%, respectively. The longest T_2 value is sufficiently long that it may be associated with free water separated from the cell wall. This component was expected since the cell wall sample was prepared in excess water. The other T_2 values correspond to water whose motion is affected by the presence of the cell wall. If the partition of water between the different components is isotope independent, we can conclude that *our bean hypocotyl cell wall preparations have an associated quantity of water with mass about 15 times that of the dry cell wall.* However, the sample underwent homogenization and lyophilization procedures during preparation so the amount of water associated with the primary cell wall of this sample may not reflect the amount of water associated with a natural bean cell wall.

A Simple Cell Wall Model. We can interpret our ^1H NMR results in terms of a simple model of the bean primary cell wall in which cellulose microfibrils are hypothesized to have a rigid outer sheath of hemicellulose II molecules. Spin-pair dipolar echo measurements indicate that this fraction makes up 64% of the primary wall mass. Cellulose itself can contribute only about $^2/_3$ of the mass of this component so, for a cellulose microfibrillar diameter of 100 Å (the lower limit compatible with our T_{1D} measurements), this hypothesized hemicellulosic layer would be about 20 Å thick and for a 400-Å microfibril the hemicellulosic layer would be 80 Å. This structure, which is considered to have cylindrical geometry, is practically rigid on the time scale of 10^{-5} s. Attached to these rigid microfibrils are pectic and hemicellulosic I molecules which make up about 36% of the mass of the cell wall. These molecules are loosely suspended in a large volume of water and undergo extensive motion on the time scale of 10^{-5} s, providing a spacious and fluid matrix.

ACKNOWLEDGMENTS

We thank F. Volke, M. Bloom, and E. Sternin for helpful discussions.

Registry No. Cellulose, 9004-34-6; hemicellulose, 9034-32-6; pectin, 9000-69-5.

REFERENCES

Abragam, A. (1961) *The Principles of Nuclear Magnetism*, Oxford University Press, London.
Ashwell, G. (1966) *Methods Enzymol. 8*, 85–95.
Atalla, R. H., & VanderHart, D. L. (1984) *Science (Washington, D.C.) 223*, 283–285.
Atalla, R. H., Gast, I. C., Sindorf, D. W., Bartuska, V. J., & Maciel, G. E. (1980) *J. Am. Chem. Soc. 102*, 3249–3251.
Bloom, M., Burnell, E. E., Roeder, S. B. W., & Valic, M. L. (1977) *J. Chem. Phys. 66*, 3012–3020.
Bloom, M., Holmes, K. T., Mountford, C. E., & Williams, P. G. (1986) *J. Magn. Reson. 69*, 73–91.
Blumenkrantz, N., & Asboe-Hansen, G. (1973) *Anal. Biochem. 54*, 484–489.
Boden, N., & Mortimer, M. (1973) *Chem. Phys. Lett. 21*, 538–540.
Brown, L. R., Bosch, C., & Wutrich, K. (1981) *Biochim. Biophys. Acta 642*, 296–312.
Carr, H. Y., & Purcell, E. M. (1954) *Phys. Rev. 94*, 630–638.
Chanzy, H., Imada, K., Mollard, A., Vuong, R., & Barnoud, F. (1979) *Protoplasma 100*, 303–316.
Davis, J. H. (1983) *Biochim. Biophys. Acta 737*, 117–171.
Fry, S. C. (1986) *Annu. Rev. Plant Physiol. 37*, 165–186.
Goldman, M. (1970) *Spin Temperature and Nuclear Magnetic Resonance in Solids*, p 300, Oxford University Press, London.
Goldman, M., & Shen, L. (1966) *Phys. Rev. 144*, 321–331.
Harai, A., Horii, F., & Kitamaru, R. J. (1980) *J. Polym. Sci. 18*, 1801–1809.
Haw, J. F., Maciel, G. E., & Schroeder, H. A. (1984) *Anal. Chem. 56*, 1323–1329.
Horii, F., Harai, A., & Kitmaru, R. (1984) *J. Carbohydr. Chem. 3*, 641–662.
James, F., & Roos, M. (1975) *Comput. Phys. Commun. 10*, 343–367.
Jeener, J., & Broekaert, P. (1967) *Phys. Rev. 157*, 232–240.
Joseleau, J. P., & Chambat, G. (1984) *Physiol. Veg. 22*, 461–470.
MacKay, A. L., Bloom, M., Tepfer, M., & Taylor, I. E. P. (1982) *Biopolymers 21*, 1521–1534.
MacKay, A. L., Tepfer, M., Taylor, I. E. P., & Volke, F. (1985) *Macromolecules 18*, 1124–1129.
Mansfield, P. (1965) *Phys. Rev. 137*, A961–A974.
McNeil, M., Darvill, A. G., Fry, S. C., & Albersheim, P. (1984) *Annu. Rev. Biochem. 53*, 625–663.
Meiboom, S., & Gill, D. (1958) *Rev. Sci. Instrum. 29*, 688–691.
Pauls, K. P., MacKay, A. L., Soderman, O., Bloom, M., Taneja, A. K., & Hodges, R. S. (1985) *Eur. Biophys. J. 12*, 1–11.
Pfeffer, P. E. (1984) *J. Carbohydr. Chem. 3*, 613–639.
Preston, R. D. (1979) *Annu. Rev. Plant Physiol. 30*, 55–78.
Sasaki, K., & Taylor, I. E. P. (1984) *Plant Cell Physiol. 24*, 989–997.
Sasaki, K., & Taylor, I. E. P. (1986) *Plant Physiol. 81*, 493–496.
Sternin, E. (1985) *Rev. Sci. Instrum. 56*, 2043–2049.
Taiz, L. (1984) *Annu. Rev. Plant Physiol. 35*, 585–657.
Taylor, I. E. P., Tepfer, M., Callaghan, P. T., MacKay, A. L., & Bloom, M. (1983) *J. Appl. Polym. Sci.: Appl. Polym. Symp. 37*, 377–384.
van Holst, G. J., Klis, F. M., Bouman, F., & Stegwee, D. (1980) *Planta 149*, 209–212.